ENGINEERING TRANSACTIONS • *Engng. Trans.* • **42**, 1–2, 107–122, 1994
Polish Academy of Sciences • Institute of Fundamental Technological Research

OPTIMAL DESIGN OF SPECIMENS FOR PURE SHEAR TESTS OF SHEET METALS

G. SOCHA (WARSZAWA)

A new type of simple specimens for experimental testing of plastic properties of sheet metals under pure shear conditions is proposed and optimized. The objectives of optimal design require possible uniformity of the shear stress distribution and possibly small effects of stress components other than σ_{12}. Computations have been performed numerically with the use of two FEM systems for 4 types of specimens, which have been used in experimental tests for determining the yield shear stress Q of sheet metals. Conventional shear stress-displacement diagrams obtained in these tests have been compared with the results of numerical calculations.

1. Introduction

When describing the deformation-induced anisotropy of sheet metals it is necessary to determine experimentally all the anisotropy coefficients which appear in the yield criterion. As the basic yield criterion for orthotropic sheet metals, HILL'S criterion ([2] and [3]) is commonly used. It can be written in the following form

$$\frac{1}{Y_x^2}\sigma_x^2 - \left(\frac{1}{Y_x^2} + \frac{1}{Y_y^2} - \frac{1}{Y_z^2}\right)\sigma_x\sigma_y + \frac{1}{Y_y^2}\sigma_y^2 + \frac{1}{Q^2}\tau_{xy}^2 = 1, \tag{1}$$

where Y_x, Y_y and Y_z are the yield stresses under uniaxial tension (compression) in directions x, y, z respectively, and Q stands for the yield stress in shear with respect to the principal axes x, y of anisotropy in the plane of the sheet. The z-axis is perpendicular to the surface of the sheet.

In most existing proposals of the yield conditions for anisotropic sheet metals, the Bauschinger effect is neglected. However, sometimes this effect is very distinctly observed in some sheet metals (see e.g. [4]). If the Bauschinger effect is to be accounted for, the yield condition for sheet metals may be written as follows ([5] and [1])

$$
(2) \qquad \frac{1}{Y_x Z_x}\sigma_x^2 - \left(\frac{1}{Y_x Z_x} + \frac{1}{Y_y Z_y} - \frac{1}{Y_z Z_z}\right)\sigma_x\sigma_y + \frac{1}{Y_y Z_y}\sigma_y^2
+ \frac{1}{Q^2}\tau_{xy}^2 + \left(\frac{1}{Y_x} - \frac{1}{Z_x}\right)\sigma_x + \left(\frac{1}{Y_y} - \frac{1}{Z_y}\right)\sigma_y = 1,
$$

where Y_x, Y_y, Y_z stand for the yield stresses of the material under uniaxial tension in the directions x, y, z, respectively, and Z_x, Z_y, Z_z are the corresponding absolute values of the yield stresses under uniaxial compressive loading. Yield stress in shear is denoted by Q. The following relation between the yield stresses must be satisfied (ref. e.g. [1]):

$$
(3) \qquad \frac{1}{Y_x} + \frac{1}{Y_y} + \frac{1}{Y_z} = \frac{1}{Z_x} + \frac{1}{Z_y} + \frac{1}{Z_z} .
$$

Some of the coefficients of plastic anisotropy , such as the yield stresses Y_x, Z_x, Y_y, Z_y, may be measured by simple uniaxial tension and compression tests. Theoretically other moduli can be deduced from the measured yield stress of specimens cut out at various angles to the x-direction and subjected to uniaxial tension (ref. HILL [2]).

It is evident that most reliable are those values of anisotropy coefficients which are measured directly. For example, the value of yield stress Z_z under simple compression in the direction across the thickness may be measured on several test-pieces cut out from the sheet made to adhere to each other by using some adhesive (ref. e.g. [8]).

More difficult is the realization of shear tests for direct determination of the yield stress in shear Q. Specimens of various shapes are used in practice for such tests. The main problem connected with shear tests is the non-homogeneous stress and strain distribution in the deformed zone. A short analysis of some specimens used by various authors is given below and, finally, a new specimen for shear tests is proposed and optimized by using the FEM technique. Practical significance of the proposed specimen is illustrated by experimental tests.

2. Method of analysis

All specimens of different types used in this work for pure shear tests were prepared from a sheet 6 mm thick of an aluminium alloy PA2 (Al-2%Mg). The stress versus plastic strain for this material under uniaxial tension is shown in Fig. 1.

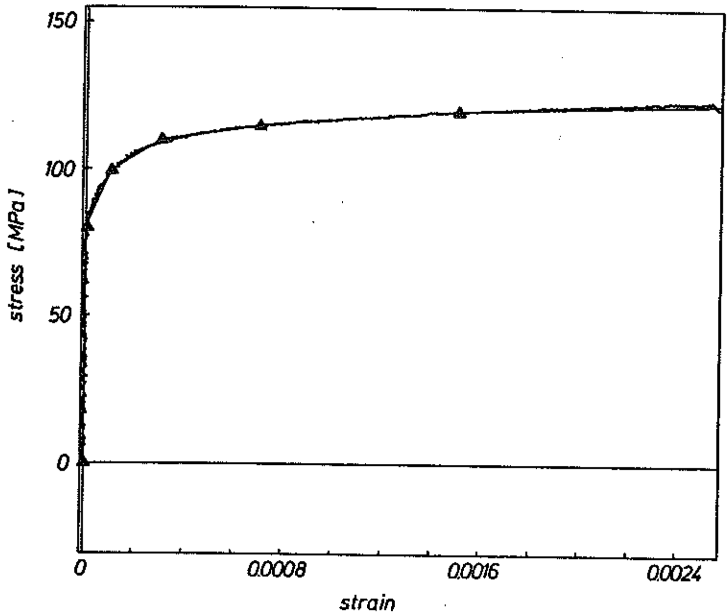

FIG. 1. Stress versus plastic strain diagram for PA2.

For all four types of shear specimens, theoretical distributions of stresses in plastic state have been calculated for various stages of deformation by means of the FEM technique. The numerical calculations have been performed with the use of the ABAQUS system. Similar computations have been made applying the COSMOS package. In the FEM calculations, the elastic-plastic model of the material was used with the plastic behaviour corresponding to the thin continuous piece-wise linear diagram shown in Fig. 1. The isotropic strain hardening hypothesis was used, assuming the isotropic expansion of the initial Huber–Mises yield surface. Material was assumed to be initially isotropic. The FEM analysis was performed in subsequent stages, initially with increasing, and after that – decreasing load acting on the specimen. Theoretical diagrams of conventional shear stress versus displacement were prepared.

For each type of specimens these theoretical diagrams were compared with the corresponding experimental diagrams. The conventional shear stresses in both the theoretical and experimental analysis were calculated from the formula

$$\sigma_{12} = \frac{P}{ht}. \tag{4}$$

Here t stands for thickness of the sheet, P is total force at a given instant and h is the width of the shearing zone indicated in Figs. 2, 4, 8, 12 (thick, solid line shows the FEM of analyzed zone of the specimen). Displacement was measured by extensometer on the base of 50 mm. For double sheared specimens only half of them was analyzed owing to the symmetry.

For the material in question the shear yield stress $Q = 52\,\mathrm{MPa}$ was indirectly measured by the uniaxial tension test of the specimen cut out from the sheet in the direction inclined by the angle of 45° to the rolling direction, similarly to the previous paper [11]. This value was later indicated on the diagrams obtained theoretically and experimentally for the specimens of various shapes.

3. Specimens of the double H type

K. Miyauchi [9] used in his test a certain type of simple shear specimen which is shown in Fig. 2. The mesh and the boundary conditions for the

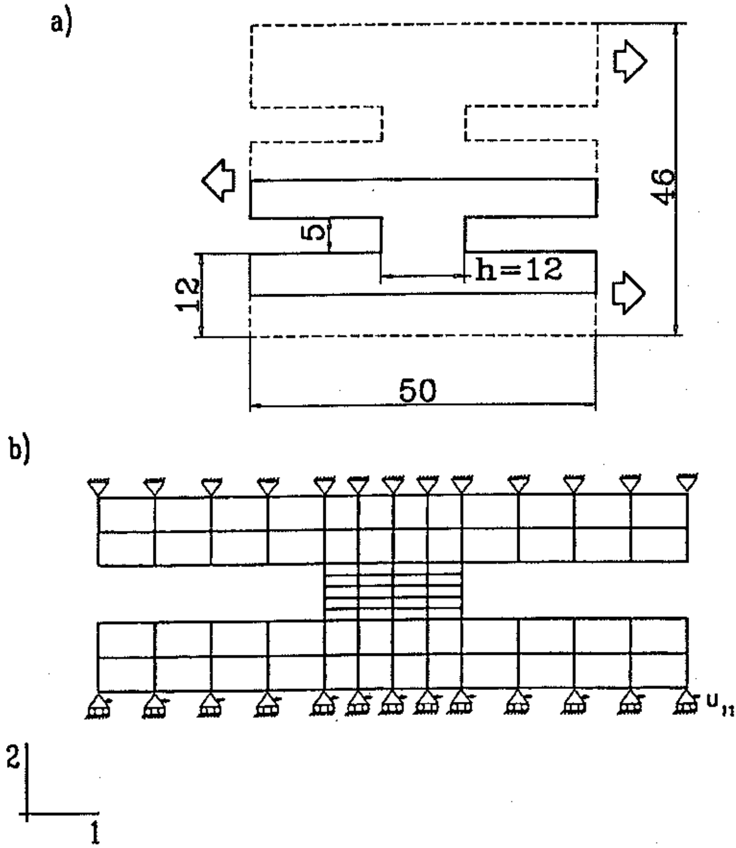

Fig. 2. Miyauchi specimen and FEM model.

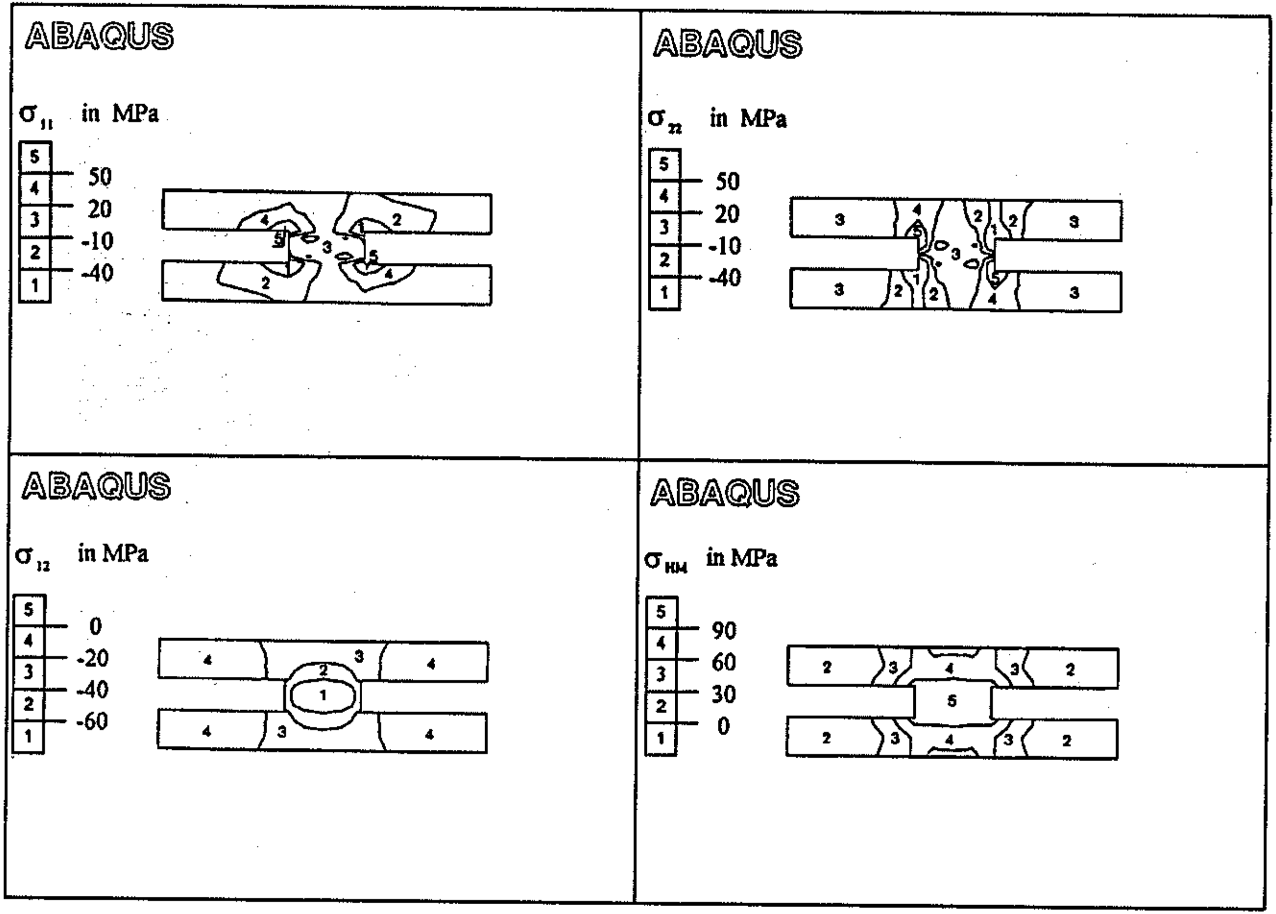

FIG. 3. Stress distribution for Miyauchi specimen.

FEM are also shown in this figure. Distributions of the calculated normal stress σ_{11} and σ_{22}, shear stress σ_{12} and the Huber–Mises equivalent stress σ_{HM} in an advanced stage of plastic deformation are shown in Fig. 3. This stress component seems to be rather uniformly distributed in the deforming region. However, it is accompanied by the normal stress component σ_{22}, as shown in Fig. 3. Thus in the deformed zone there is a complex non-homogeneous stress state resulting from the simultaneous shearing and bending, although the contribution of bending is rather small. It is also difficult to realize the boundary conditions introduced in FEM during the experimental test. Special grips are necessary to load the specimen and minimize the effect of bending.

4. Other specimens used for shear tests of sheet metals

Another type of specimens for shear tests was used by Sato *et al.* [10]. Preparation of such specimens is simple and standard grips of any testing machine may be used to hold the specimen. Specimen and FEM model are shown on Fig. 4. The specimen proved to be rather well designed. The propagations of plastic zones during the loading process and the stress distribution in the working area were analysed by the finite elements technique.

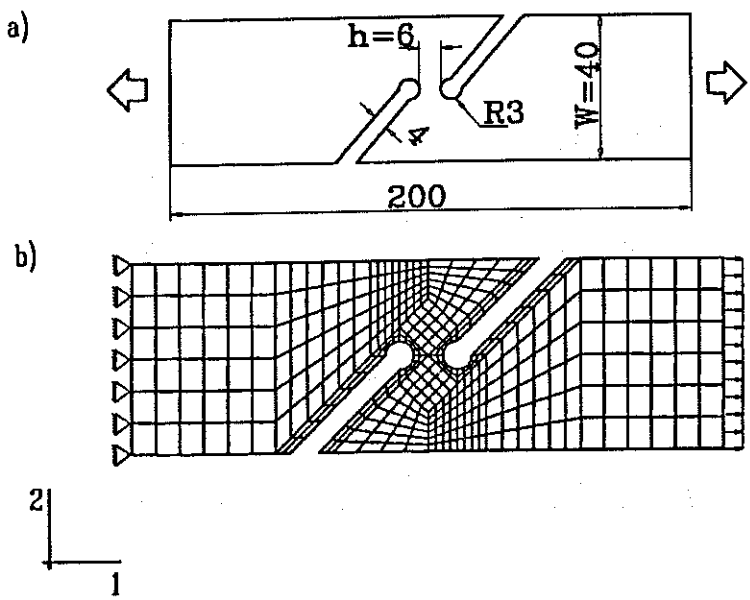

FIG. 4. Sato specimen and FEM model.

In Fig. 5 are demonstrated the calculated boundaries of plastic zones at different stages of elongation of the specimen. Distributions of all three stress components and the Huber - Mises equivalent stress corresponding to the stage IV from Fig. 5 are shown in Fig. 6. It can be seen from that figure that in the narrowest zone between the boundaries of the holes the stress state is close to the pure shear state. This result has been obtained for the dimensions ratio $W/h = 7$, although the authors of the paper [10] suggest, on the basis of their experimental analysis, that to obtain the pure shear conditions this ratio should be of the magnitude $W/h = 25$. The presented calculations do not support such a strong requirement.

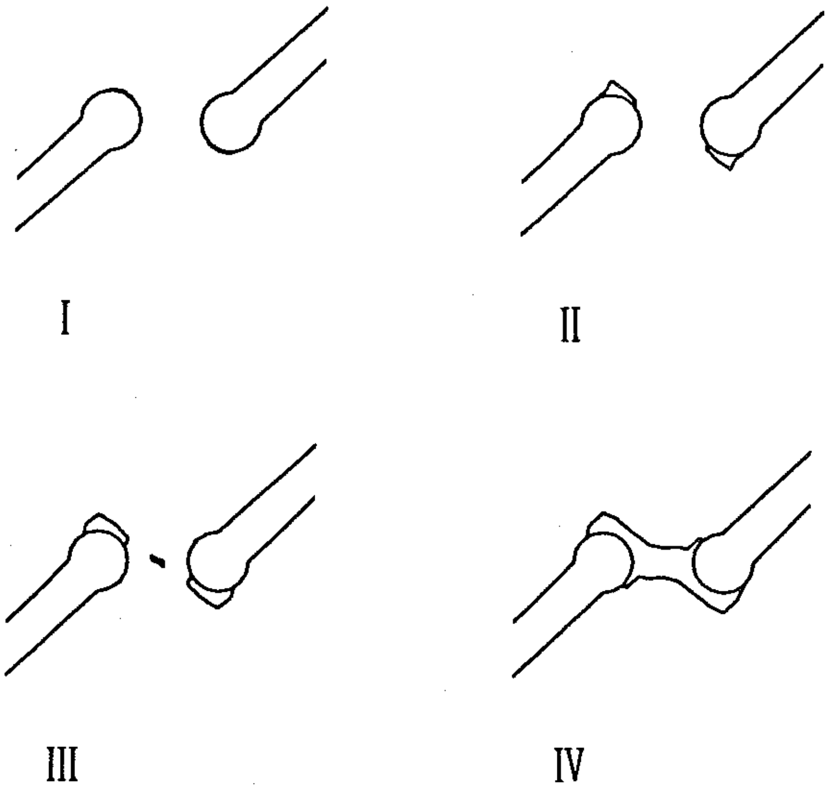

FIG. 5. Plastic zone propagation for Sato specimen.

The main disadvantage of using specimens of the type shown in Fig. 4 is connected with the non-uniform stress distribution in their end parts where they are held in grips (asymmetry of loading). Such asymmetry makes the stress distribution dependent on the type of grips that are used to hold the specimen. For larger deformations the eccentric tension in the end parts causes local bending and appearance of considerable tensile stress in the

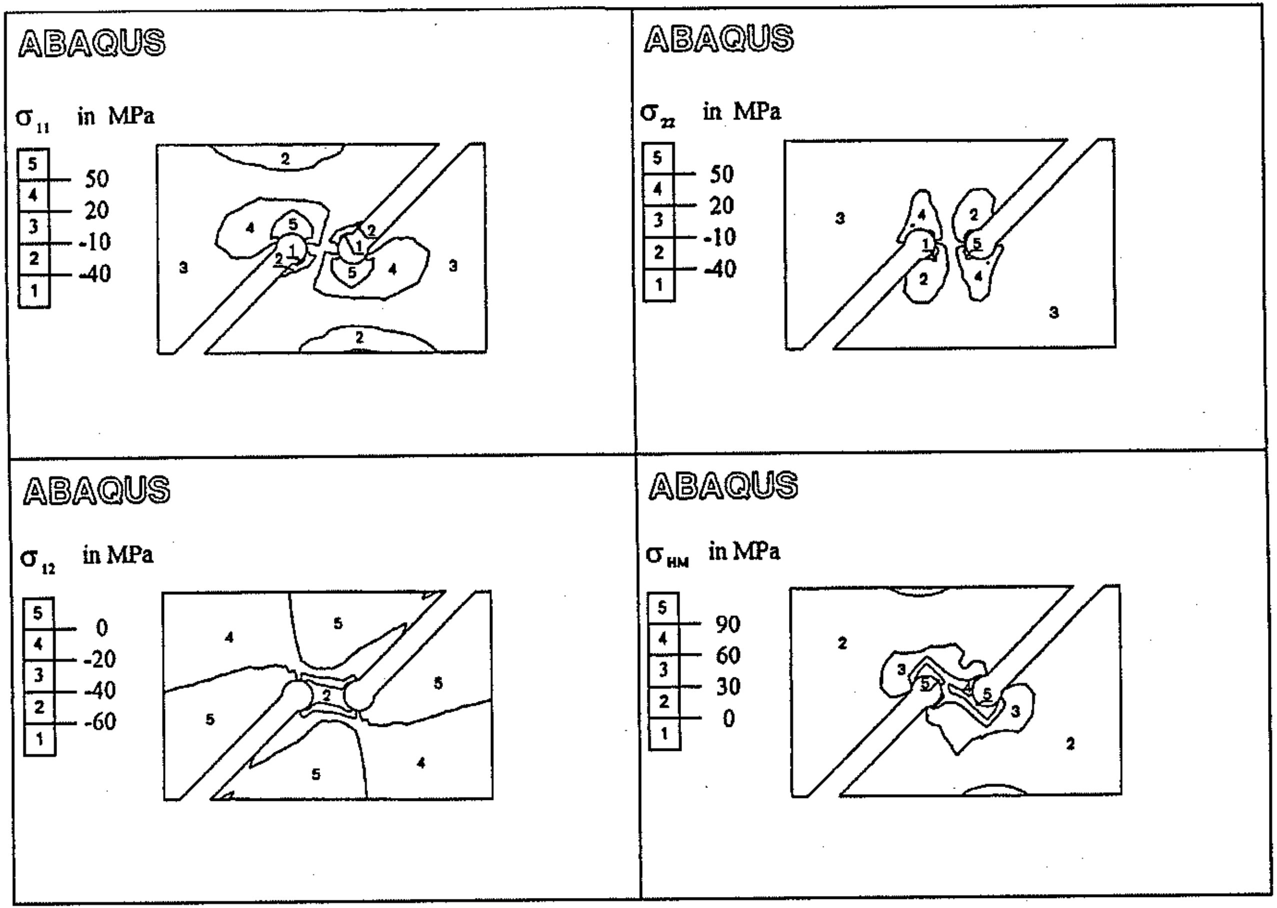

FIG. 6. Stress distribution for Sato specimen.

shear zone (ref. [10]). This effect can be easily observed in Fig. 7 as the difference between the experimental curve and the result of FEM computations. In these computations, the boundary conditions impossible to realize during the experiment (uniformly distributed pressure) have been introduced (Fig. 4). For comparison, the yield stress in shear $Q = 52\,\mathrm{MPa}$ obtained previously by a non-direct experimental measurements is shown in Fig. 7. It is seen how difficult it would be to estimate the value of Q from the direct experiment by applying a specimen of the type shown in Fig. 4.

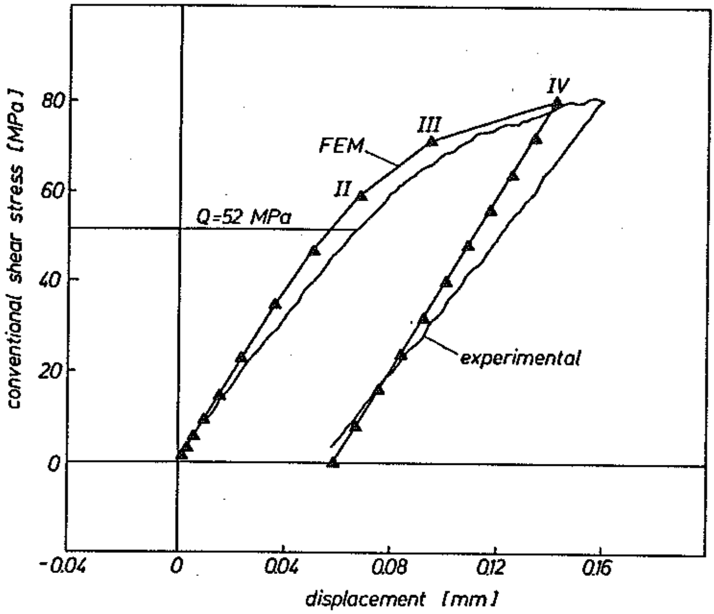

FIG. 7. Conventional shear stress – displacement diagram for Sato specimen.

5. A NEW SYMMETRICAL TYPE OF SPECIMENS FOR PURE SHEAR TESTS

To minimize the effect of the non-symmetrical loading, new types of symmetrical specimens for pure shear tests are proposed and analyzed. Two types A and B of the specimen design were analyzed. Different variants of the relation between the dimensions have been numerically analyzed. Boundary conditions assumed in the FEM calculations are similar to those in the previous section.

For the specimen of the type A shown in Fig. 8, the most uniform stress distribution in the deformed zone was found for the relation of dimensions $h/a = 2$. The FEM mesh for the calculations is also shown in Fig. 8. Four stages of the calculated propagation of plastic zones are presented in Fig. 9.

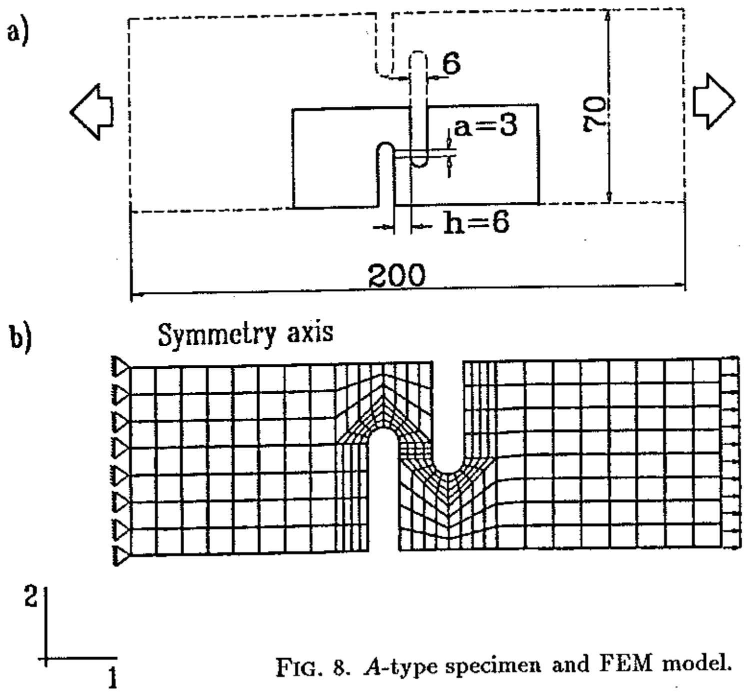

FIG. 8. *A*-type specimen and FEM model.

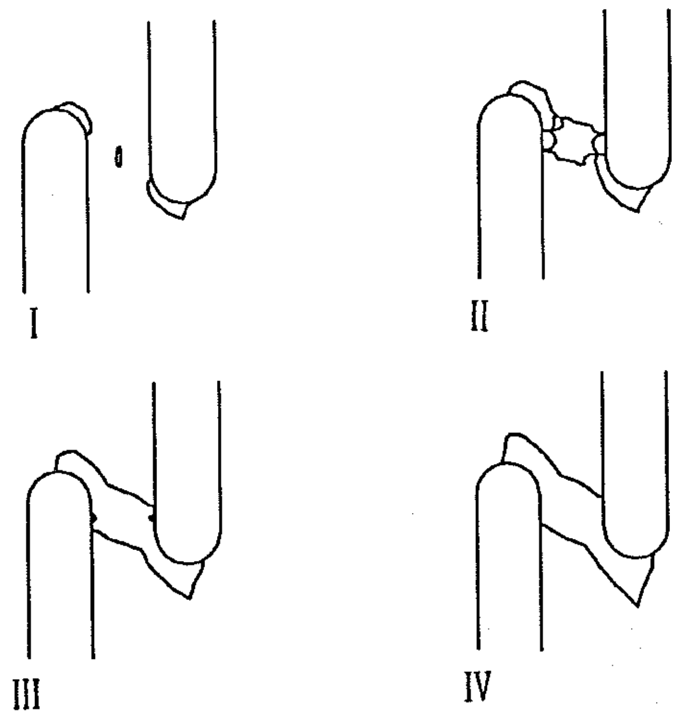

FIG. 9. Plastic zone propagation for *A*-type specimen.

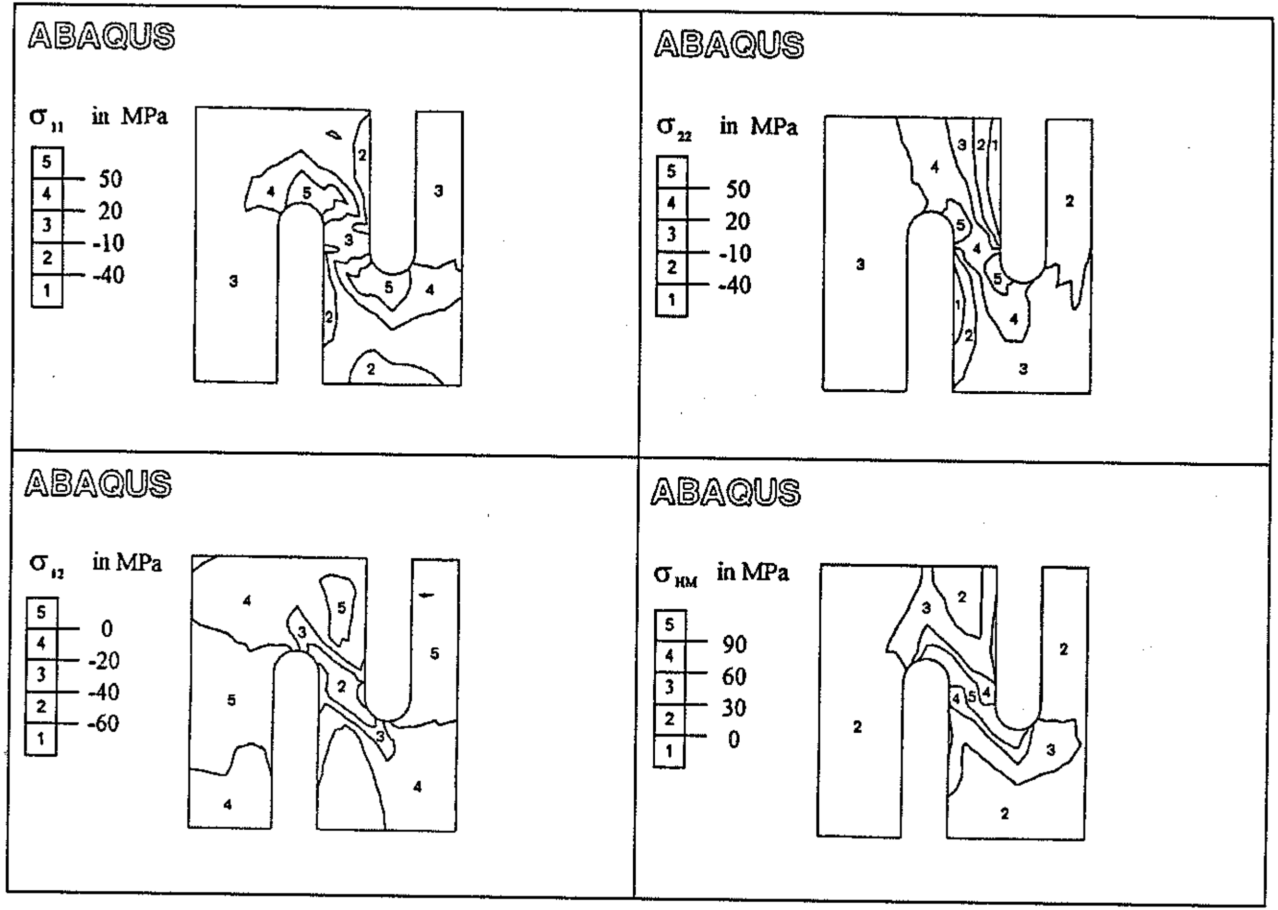

FIG. 10. Stress distribution for *A*-type specimen.

Although the shear stress distribution is rather uniform in the deforming zone, the normal stress component σ_{22} reaches the value of 50 MPa as shown in Fig. 10. This value is comparable with the value of the shear stress there. Thus the bending factor is evidently too large in symmetrical specimens of the type A. The comparison of experimental and calculated diagram of conventional shear stress versus displacement is presented in Fig. 11. The previous indirectly measured value $Q = 52$ MPa is shown in the figure for comparison. It is seen that estimation of the value of Q from the experimental curve in Fig. 11 would be very uncertain.

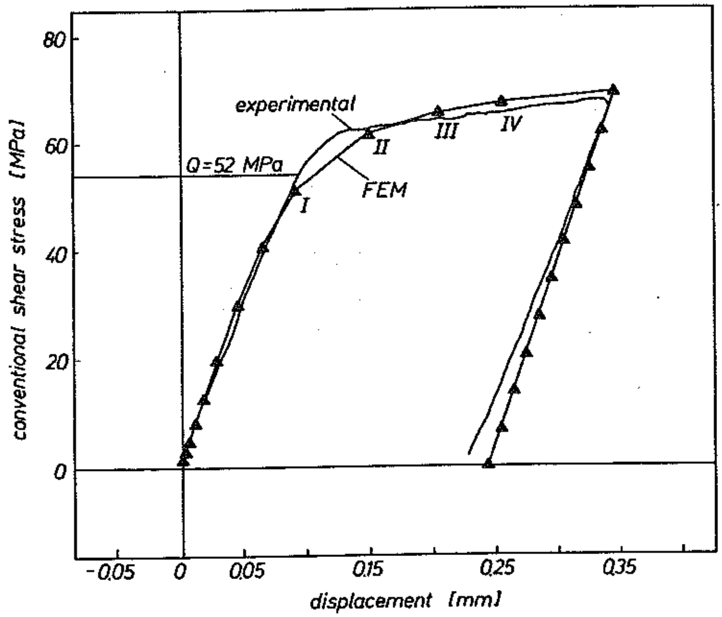

FIG. 11. Conventional shear stress – displacement diagram for A-type specimen.

To minimize the influence of bending in the deforming zone, a slightly modified specimen of the type B was analyzed using the mesh shown in Fig. 12. The stress distributions for various stages of deformation have been calculated by the FEM technique with the use of the ABAQUS system. The propagation of plastic zones for various stages of deformation is shown in Fig. 13.

The calculated distribution of shear stress σ_{12} corresponding to the stage IV (ref. Fig. 13) of plastic deformation is shown in Fig. 14. It is close to the uniform distribution along the line $C - C$. Note that now the normal stress σ_{22} resulting from the additional bending is smaller than that in the specimen of the type A.

In Fig. 15 are presented the diagrams of conventional shear stress ver-

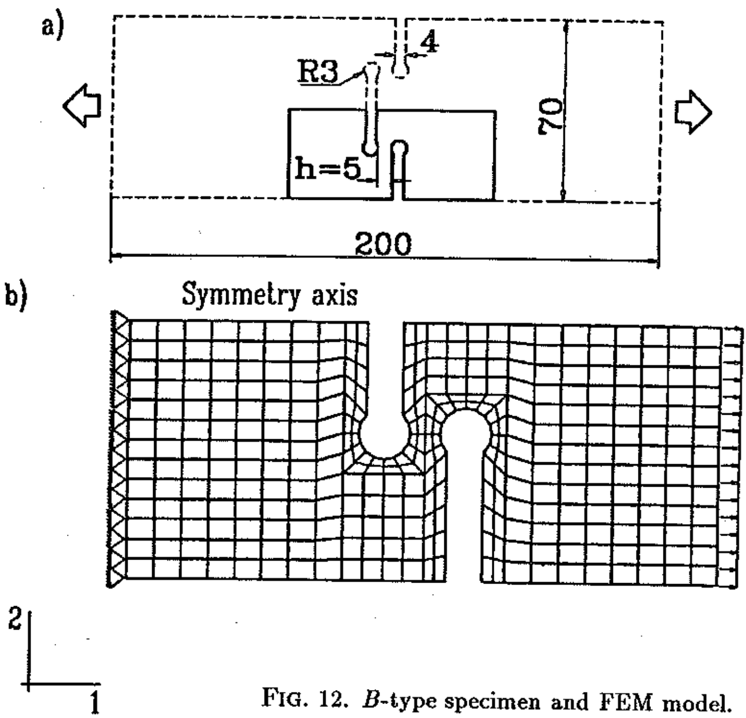

FIG. 12. *B*-type specimen and FEM model.

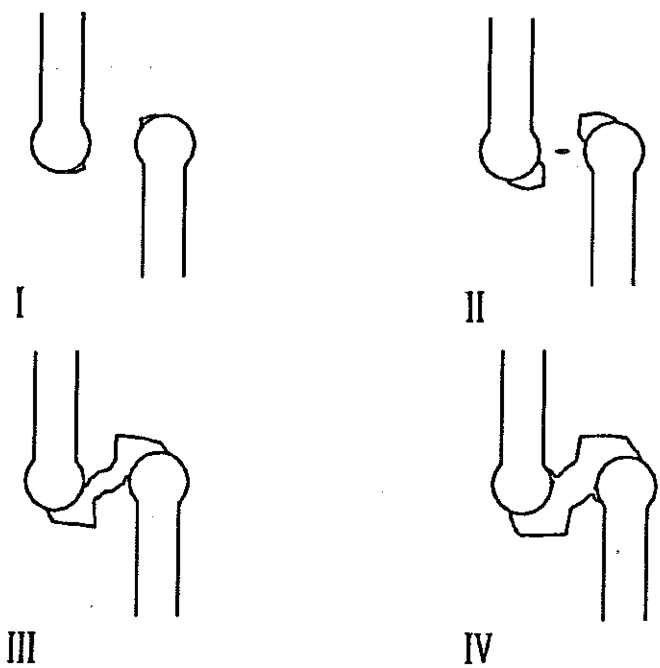

FIG. 13. Plastic zone propagation for *B*-type specimen.

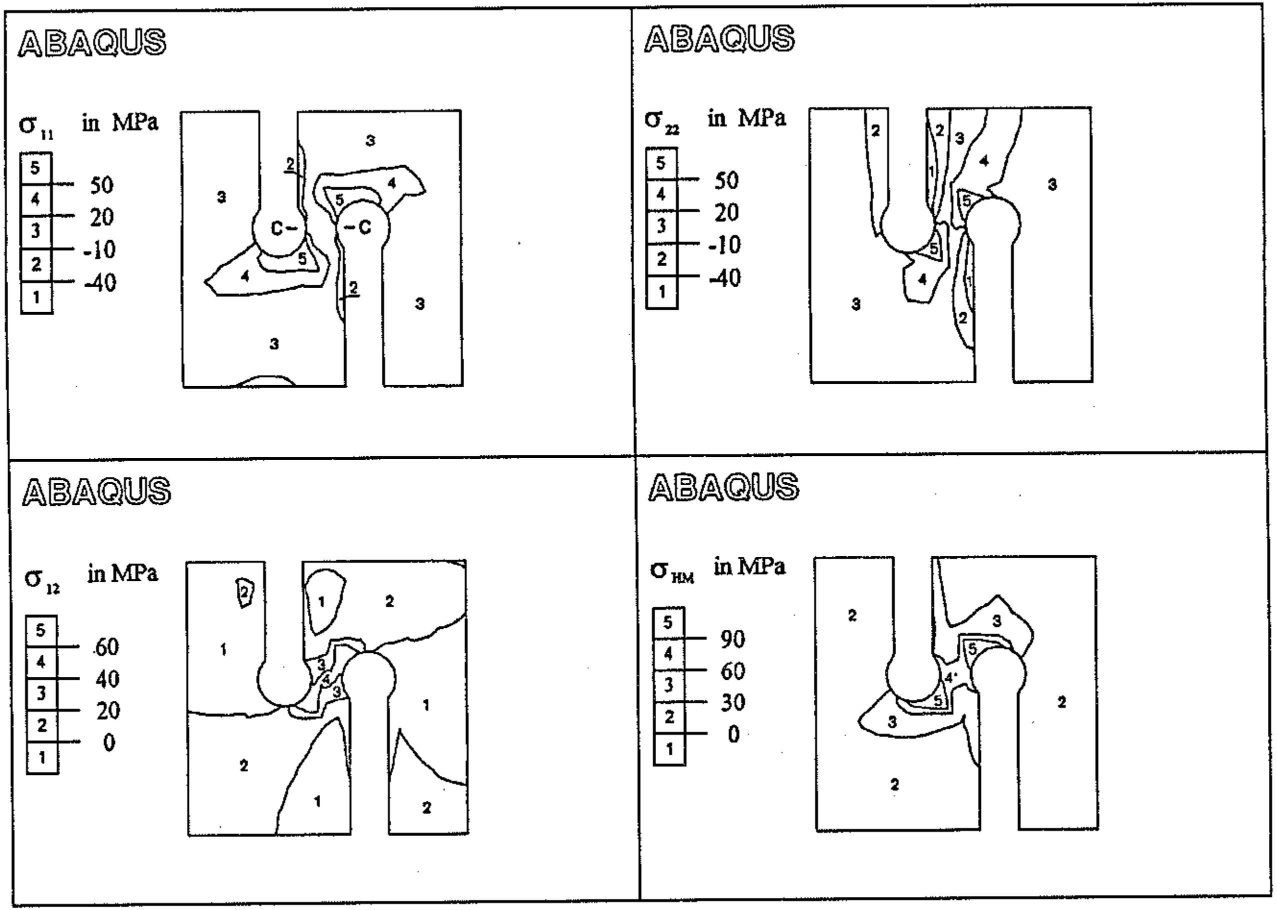

FIG. 14. Stress distribution for *B*-type specimen.

sus elongation of the specimen resulting from the theoretical calculations and from the experimental test. The consecutive stages of plastic deformation corresponding to those shown in Fig. 13 are indicated on the theoretical curve. Also in the present case the previous indirectly measured yield stress in shear $Q = 52\,\mathrm{MPa}$ is shown for comparison. It is evident that direct estimation of this yield stress from the experimental curve would be of questionable accuracy.

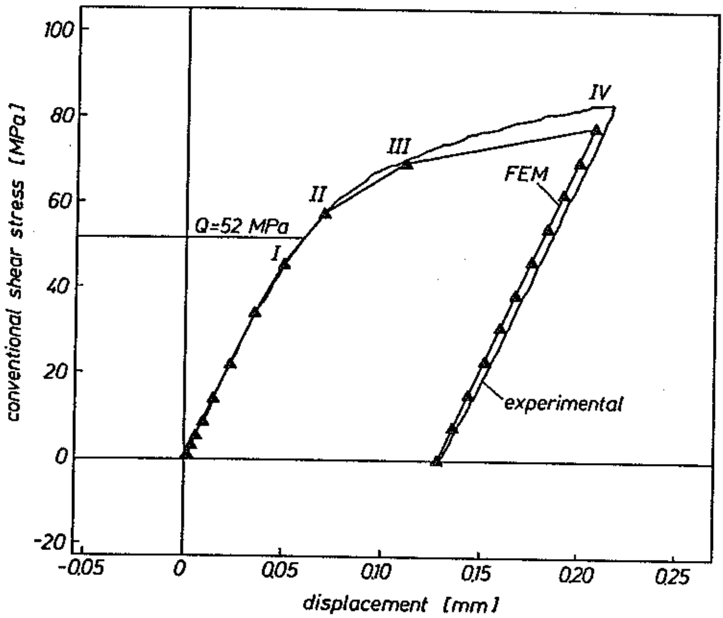

FIG. 15. Conventional shear stress – displacement diagram for B-type specimen.

6. Conclusions

The theoretical and experimental study presented above clearly indicates that direct measurement of the yield stress in shear of sheet metals is connected with some difficulties concerning the interpretation of experimental results. The value of shear stress calculated by dividing the total force by the area of the working cross-section gives only some averaged values of the non-uniformly distributed stresses. Additionally, the cross-section with most uniform distribution of shear stress is inclined at some angle to the load direction. Even more difficult is the problem of measuring the shear strains, since these strains are also non-uniformly distributed.

The specimens proposed in this paper have several advantages. The boundary conditions introduced in FEM computations are easy to apply on testing machine (ordinary grips can be used) and, what is very important, the stress distributions are symmetrical to the loading direction (there is no unbalanced bending moment). The stress distribution in deforming zone is almost uniform, and there is a small contribution of stress components other than σ_{12} for the B-type specimen. Finally, those specimens can be easily machined from the metal sheet.

References

1. W. Szczepiński, *On deformation-induced plastic anisotropy of sheet metals*, Arch. Mech., **45**, 1, 3–38, 1993.
2. R. Hill, *A theory of yielding and plastic flow of anisotropic metals*, Proc. Roy. Soc. London, **A 193**, 281–297, 1948.
3. R. Hill, *The mathematical theory of plasticity*, Oxford at the Clarendon Press, 1956.
4. A. Litewka, *Plastic flow of anisotropic aluminium alloy sheet metals*, Bull. Acad. Polon. Sci., **25**, 475–484, 1977.
5. T. Ota, A. Shindo, F. Fukuoka, *A consideration on anisotropic yield criterion*, Proc. 9th Jap. Nat. Congr. Appl. Mech, 117–120, 1959.
6. J. Woodthrope and J. Pearce, *The anomalous behaviour of aluminium sheet under balanced biaxial tension*, Intern. J. Mech. Sci, **12**, 341–347, 1970.
7. R. Hill, *Theoretical plasticity of textural aggregates*, Math. Proc. Cambridge Phil. Soc., **85**, 179–191, 1979.
8. M. Gotoh, *A theory of plastic anisotropy based on a yield function of fourth order (plane stress state)* – I, Intern. J. Mech. Sci., **19**, 505–512, 1977.
9. K. Miyauchi, *On a simple shear deformation*, English text reprinted from Scientific Papers of the Institute of Physical and Chemical Research (Rikagaku Kenkyusho, Wako-shi, Saitama, Yapan), **81**, 57–67, 1987.
10. K. Sato, Y. Miyaki, Y. Toyabara, *Inplane single shear deformation of Ti-6Al-YV alloy sheet under transformational superplasticity condition*, Proc. 13th Riso International Symposium on Materials Science, Riso Nat. Lab. Roskilde, 423–429, Denmark 1992.
11. G. Socha, W. Szczepiński, *On experimental determination of the coefficients of plastic anisotropy in sheet metals*, [in press].

POLISH ACADEMY OF SCIENCES
INSTITUTE OF FUNDAMENTAL TECHNOLOGICAL RESEARCH.

Received November 5, 1993.